Electronic Supplementary Information (ESI)

Bifunctional pyrazolate-carboxylate ligands for isoreticular cobalt and zinc MOF-5 analogs with magnetic analysis of the {$Co_4(\mu_4\text{-}O)$} node

Christian Heering,[a] Ishtvan Boldog,[a] Vera Vasylyeva,[a] Joaquín Sanchiz,*[,b] Christoph Janiak*[,a]
[a] Institut für Anorganische Chemie und Strukturchemie, Universität Düsseldorf, D-40204 Düsseldorf, Germany. Fax: +49 211 8112287;
E-mail: christian.heering@uni-duesseldorf.de
E-mail: ishtvan.boldog@uni-duesseldorf.de
E-mail: vira.vasylyeva@uni-duesseldorf.de
E-mail: janiak@uni-duesseldorf.de

[b] Departamento de Química Inorgánica, Universidad de La Laguna, La Laguna 38206, Tenerife, Spain
E-mail: jsanchiz@ull.es

Content: **page**

Experimental Section

Materials

1*H*-Pyrazole-4-carboxylic acid was purchased in 97 % grade from Carbolution.

Solvents were p.a. grade.

Methods

Melting point measurement was performed in an open capillary using a Büchi-B450 apparatus. FT-IR measurements were carried out on a Bruker TENSOR 37 IR spectrometer at ambient temperature in the range of 4000 to 500 cm^{-1} either in a KBr pellett or with an ATR unit (Platinum ATR-QL, Diamond). ^{1}H and ^{13}C spectra were recorded on Bruker Avance DRX-200 Bruker Avance DRX-500 instruments respectively. High resolution mass spectra (ESI) were collected with a UHR-QTOF maXis 4G from Bruker Daltonics.

Elemental (CHN) analyses were carried out on a Perkin Elmer CHN 2400.

Thermogravimetric analysis (TGA) was performed on a Netzsch TG 209 F3 at 10 °C/min heating rate using corundum sample holders and nitrogen as carrier gas.

Synthesis of ligands

3,5-Dimethyl-1*H*-pyrazole-4-carboxylic acid (HMe_2pzCO_2H)

This compound has been synthesized according to literature procedures, following those of Knorr and Rosenberg (Fig. S1).[1] Diacetyl ethylcacetate (**I**) was obtained in 45% yield in a first step by the method of Spassow.[2] Intermediate **I** with hydrazine monohydrate gave the ethyl ester of HMe_2pzCO_2H, **II** in 80% yield in water. As the final step the ester was hydrolyzed to give the product in 90% yield. FTIR (ATR): 3007, 2919, 1700, 1542, 1505, 1477, 1420, 1391, 1368, 1309, 1171, 997, 950, 816, 803, 745, 712, 671, 617 cm^{-1} (Fig. S2)

^{1}H-NMR ($CDCl_3$, 500 MHz): δ/ppm = 1.88 (s, 6H, CH_3), 12.8 (s, COOH) (Fig. S3).

^{13}C-NMR ($CDCl_3$, 500 MHz): δ/ppm = 40.0 (s, *C*H_3), 129.0 135.5 143.5 (pyrazole C's) 167.8 (s, *C*OOH) (Fig. S4).

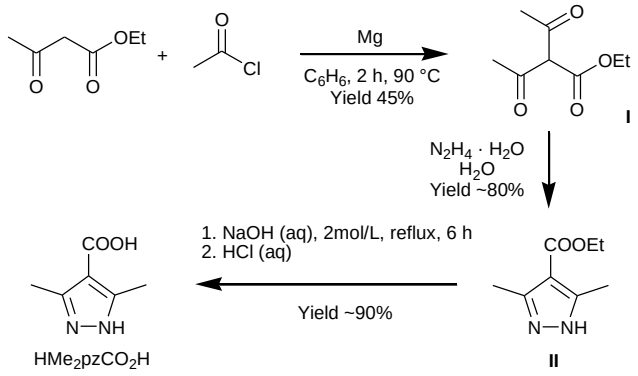

Fig. S1. Synthesis for 3,5-dimethyl-1*H*-pyrazole-4-carboxylic acid (HMe_2pzCO_2H).

1 G. D. Rosengarten, *Justus Liebigs Annalen der Chemie* **1894**, *279*, 237–243.
2 A. Spassow, *Organic Syntheses* **1955**, *3*, 390.

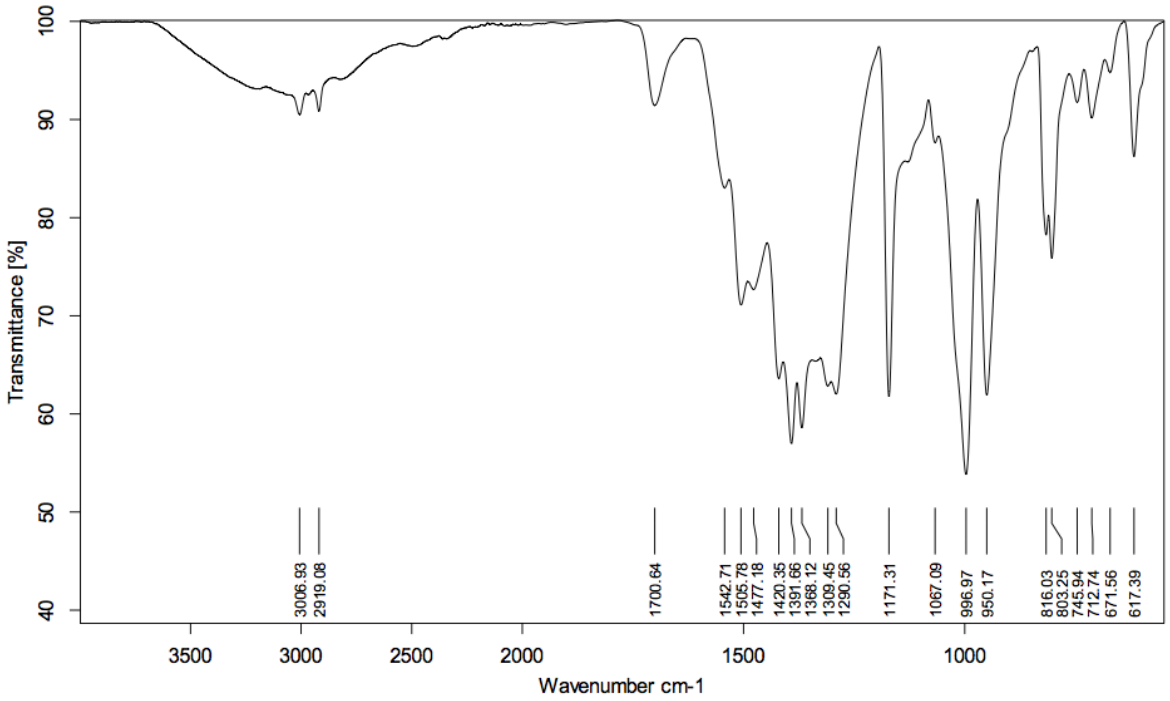

Fig. S2. FTIR (ATR) of 3,5-dimethyl-1*H*-pyrazole-4-carboxylic acid (HMe_2pzCO_2H).

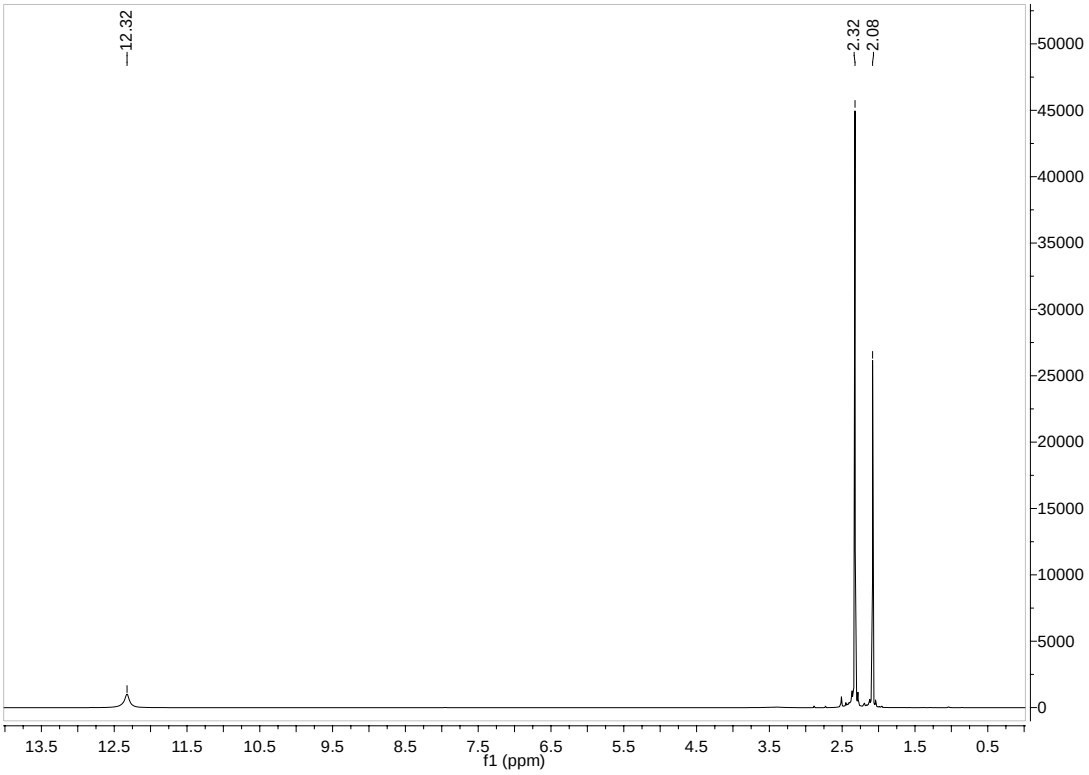

Fig. S3. ^1H NMR (in $CDCl_3$) of 3,5-dimethyl-1*H*-pyrazole-4-carboxylic acid (HMe_2pzCO_2H).

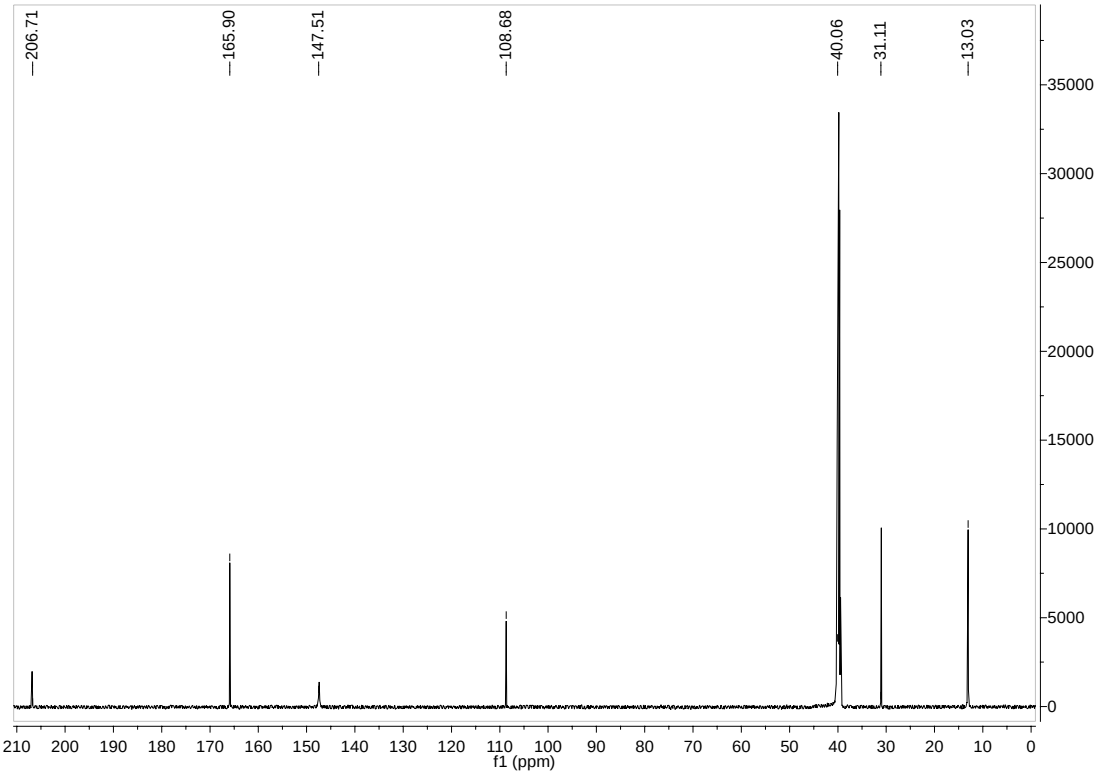

Fig. S4. ^{13}C NMR (in $CDCl_3$) of 3,5-dimethyl-1*H*-pyrazole-4-carboxylic acid (HMe_2pzCO_2H).

3,5-Dimethyl-4-(4-carboxyphenyl)-1*H*-pyrazole, 4-(3,5-dimethyl-1H-pyrazol-4-yl)benzoic acid ($HMe_2pzC_6H_4CO_2H$) (see Fig. S5)

a) 3-(4-Carboxyphenyl)-2,4-pentanedione

In a first step 3-(4-carboxyphenyl)-2,4-pentanedione (**III**) was synthesized in a copper-catalyzed reaction with L-proline.[3] In a 0.5 L round-bottom flask 12 g (48 mmol) of 4-iodobenzoic acid and 14 g (threefold excess, 144 mmol) of 2,4 pentanedione were dissolved in 250 mL of dimethylsulfoxide (DMSO). After addition of 1.8 g (9.5 mmol) CuI and 2.2 g (19 mmol) L-proline the solution turned from yellow to bluish-green and 32.2 g (0.24 mol) of K_2CO_3 was added as a base. Under constant stirring under nitrogen atmosphere the reaction mixture was heated to 90 °C and kept at this temperature for 24 h. After cooling down to room temperature the dark solution was poured into 250 mL water and acidified with aqueous 12 mol/L HCl to pH 3. The solution became yellow again and was then extracted three times by 25 mL portions of ethyl acetate. The separated organic phase was treated with 15 mL of brine (saturated solution), separated again and dried over Na_2SO_4. After evaporation of the solvent the brown and oilish residue was poured into water, yielding 4.2 g of a brown solid compound (40 % based on 4-iodobenzoic acid).

3 Y. Jiang, N. Wu, H. Wu, M. He, *ChemInform* **2006**, 37.

mp = 95 °C (lit. value unknown)

FTIR (ATR): 2832, 2724, 2667, 2547, 1928, 1803, 1672, 1582, 1482, 1422, 1391, 1317, 1292, 1271, 1178, 1124, 1107, 1052, 1003, 929, 847, 807, 750, 682, 655, 625, 563 cm^{-1} (Fig. S6)

^{1}H-NMR (DMSO-d_6, 500 MHz): δ/ppm = 1.88 (s, 6H, CH_3CO), 5.5 (s, 1H, acidic H -CO-C*H*-CO-), 7.43, 7.98 (2xd, 4H, C_6H_4), 13.0 (s, COOH) (Fig. S7).

^{13}C-NMR (DMSO-d_6, 500 MHz): δ/ppm = 40.0 (s, CH_3), 101.6 (s, -CO-*C*H-CO-), 130-137 (aromatic C's), 167.3 (*C*=O).

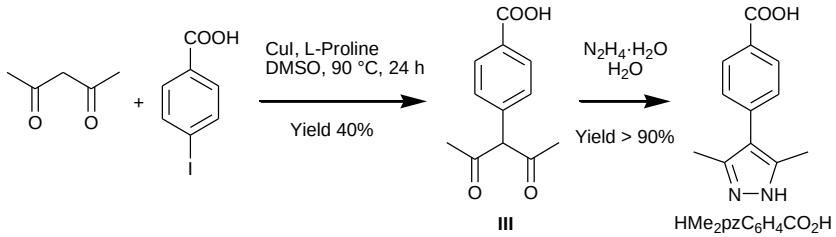

Fig. S5. Synthesis of 3,5-dimethyl-4-(4-carboxyphenyl)-1*H*-pyrazole, 4-(3,5-dimethyl-1H-pyrazol-4-yl)benzoic acid ($HMe_2pzC_6H_4CO_2H$).

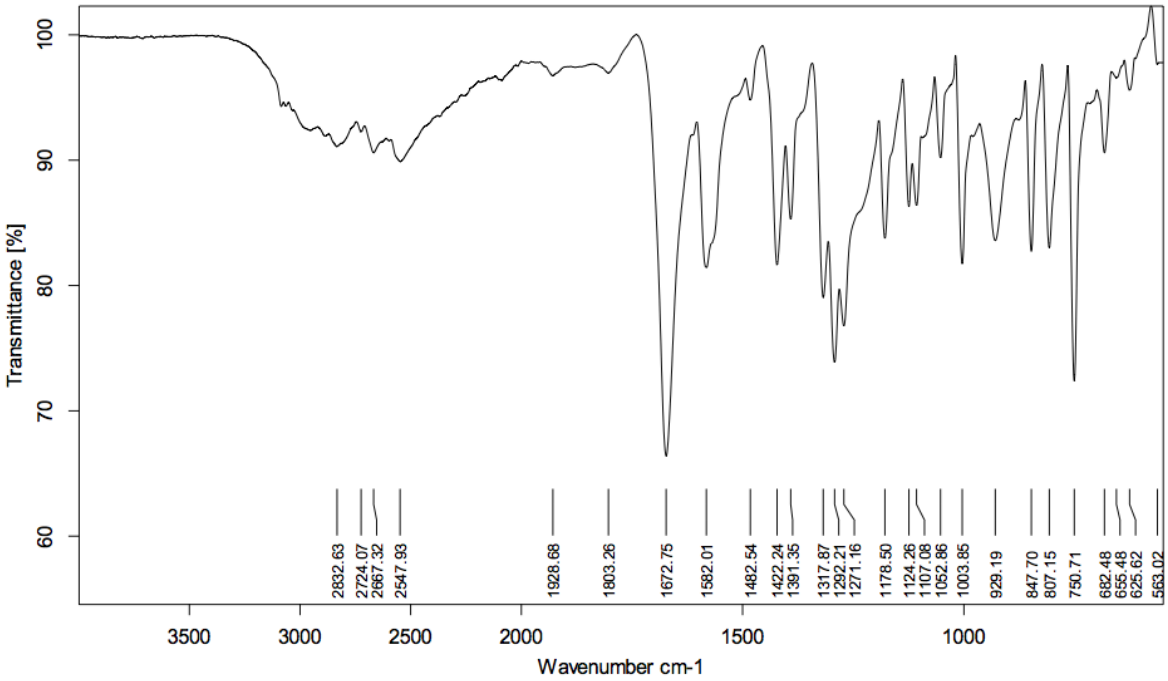

Fig. S6. FTIR (ATR) of 3-(4-carboxyphenyl)-2,4-pentanedione (**III**).

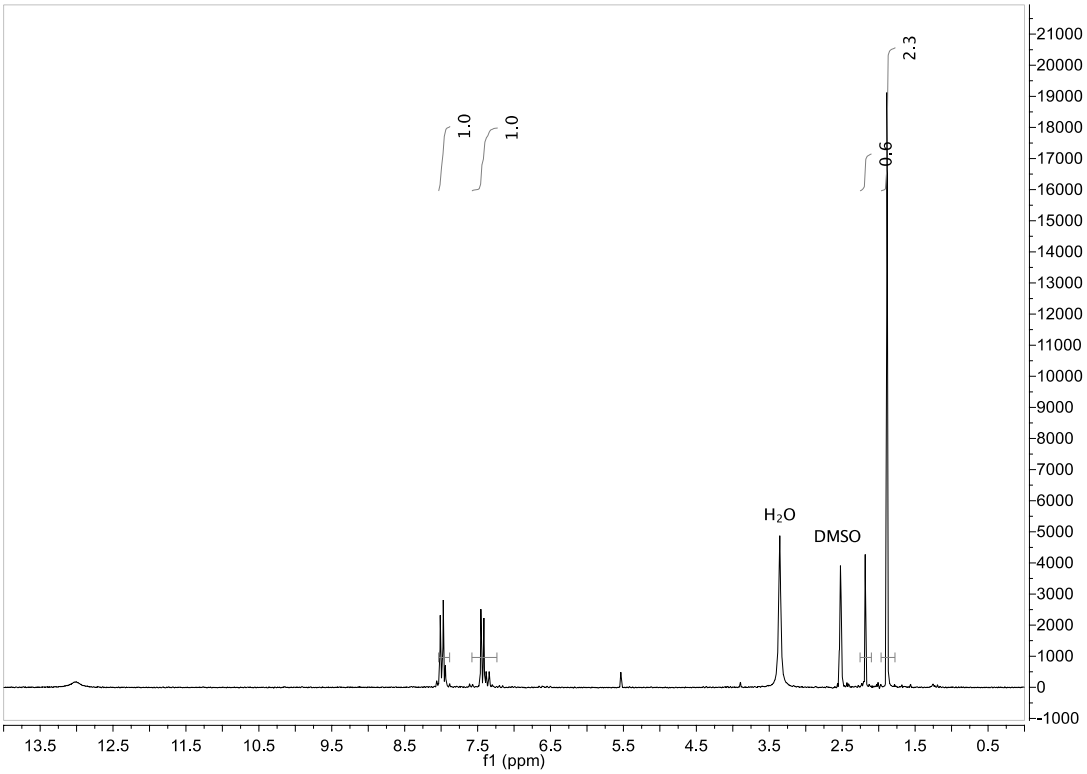

Fig. S7. ^{1}H NMR (in DMSO-d_6) of 3-(4-carboxyphenyl)-2,4-pentanedione (**III**).

b) 3,5-Dimethyl-4-(4-carboxyphenyl)-1*H*-pyrazole, 4-(3,5-dimethyl-1*H*-pyrazol-4-yl)benzoic acid ($HMe_2pzC_6H_4CO_2H$)

The pentanedione **III** was suspended in 20 mL of water in a 50 mL round-bottom flask. Under constant stirring 75 mg (1.5 mmol) of hydrazine monohydrate dissolved in 5 mL of water was added dropwise to the flask. After one hour the clear solution was treated with concentrated HCl (12 mol/L) to bring the mixture to a pH value of 3. The white precipitate was separated by filtration, dried under vacuum and washed with 15 mL of aceton to give 0.28 g of pure product (> 90 % based on **III**).

mp > 295 °C (decomp.). Calcd. for $C_{12}H_{12}N_2O_2$ (216.24 g/mol) C 66.65, H 5.59, N 12.96; found C 65.91, H 5.71, N 12.64%.

FTIR (ATR): 3276, 2988, 2933, 2438, 1942, 1677, 1607, 1412, 1254, 1174 cm^{-1} (see Fig. S8).

^{1}H-NMR (DMSO-d_6, 500 MHz): δ/ppm = 2.25 (s, 6H, CH_3), 7.42 (d, 2H), 7.98 (d, 2H), 13 (s, br, COOH) (Fig. S9).

^{13}C-NMR (DMSO-d_6, 500 MHz): δ/ppm = 11.87 (s, *C*H_3), 124-130 (aromatic C's), 139.27 (s, *C*-N), 167.85 (s, *C*OOH) (Fig. S10).

ESI-MS (neg.) 215.08234 $[M\text{-}H^+]^-$, calcd. $^{12}C_{12}H_{11}N_2O_2$: 215.08260 (100%).

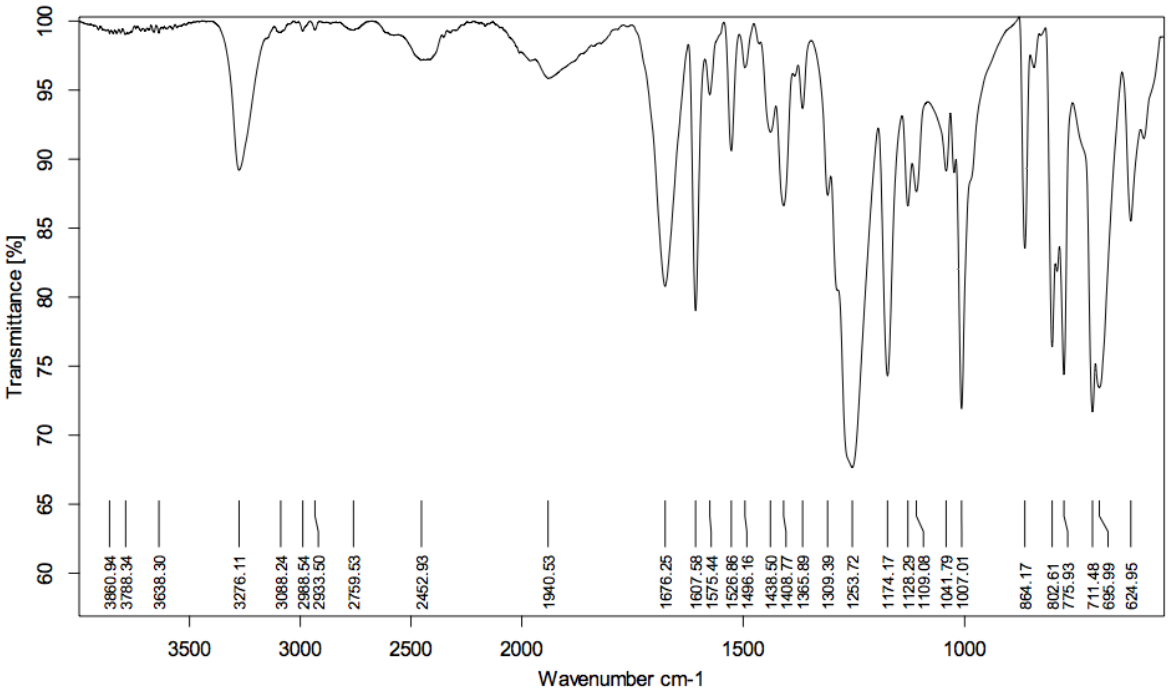

Fig. S8. FTIR (ATR) of 4-(3,5-dimethyl-1H-pyrazol-4-yl)benzoic acid $HMe_2pzC_6H_4CO_2H$.

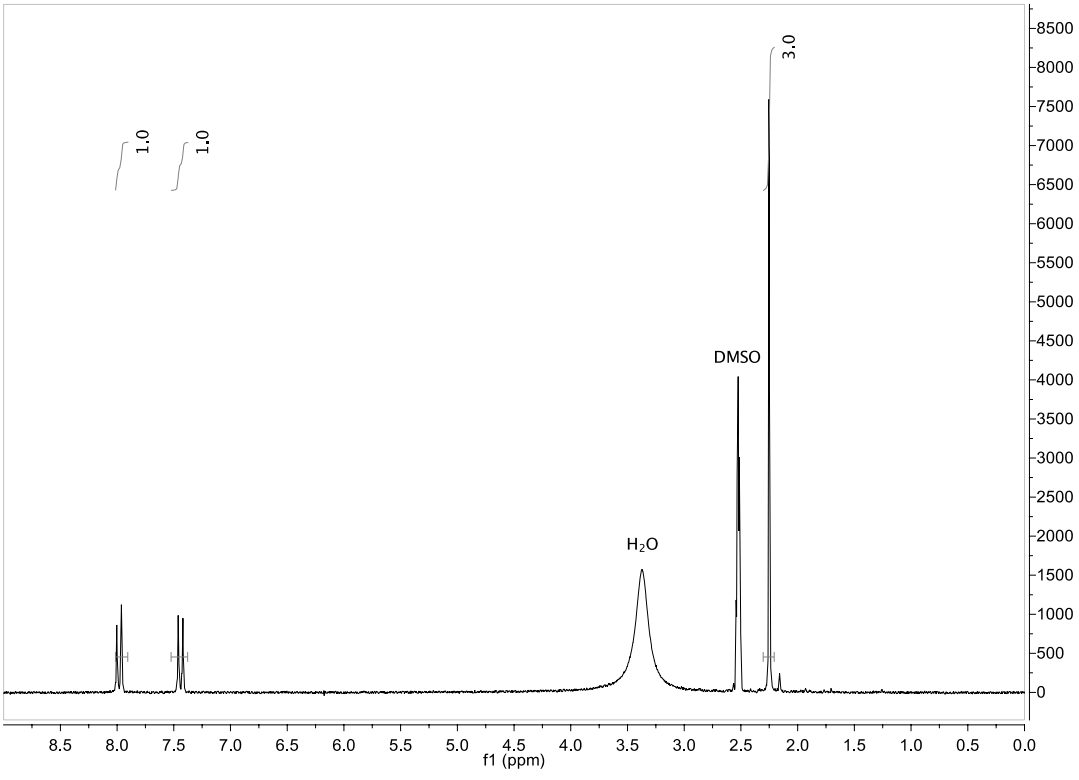

Fig. S9. ^{1}H-NMR (DMSO-d_6) of 4-(3,5-dimethyl-1H-pyrazol-4-yl)benzoic acid $HMe_2pzC_6H_4CO_2H$.

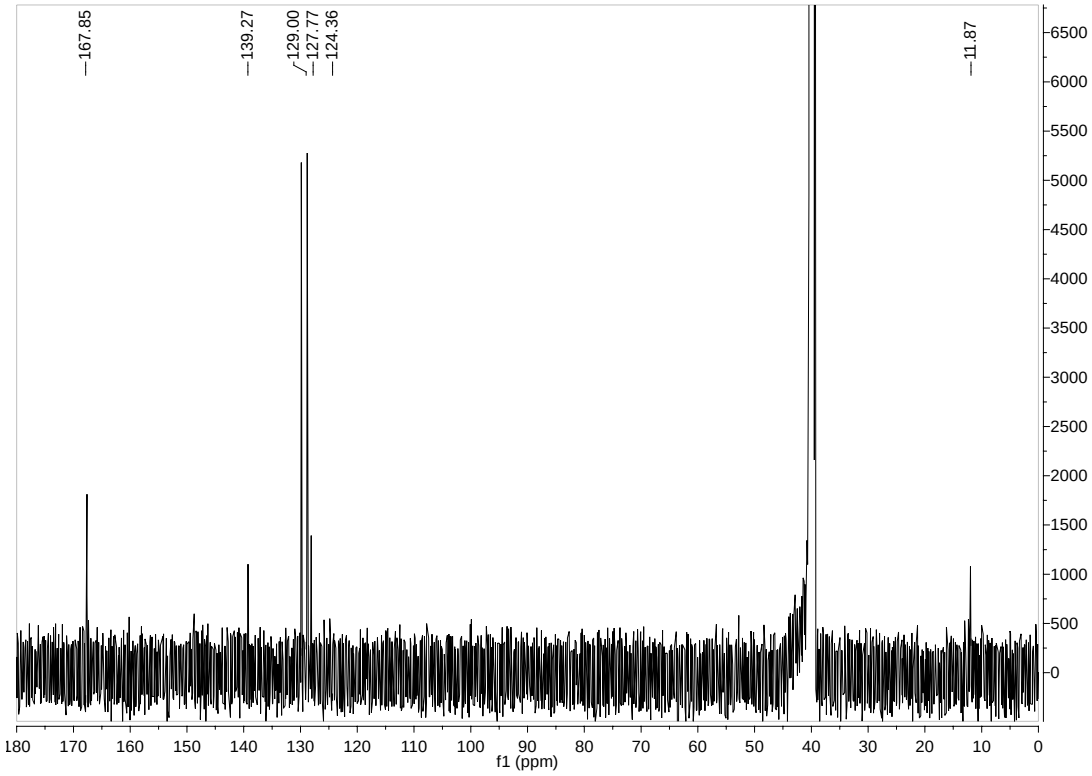

Fig. S10. ^{13}C-NMR (DMSO-d_6) of 4-(3,5-dimethyl-1H-pyrazol-4-yl)benzoic acid $HMe_2pzC_6H_4CO_2H$.

Synthesis of complexes

{[$Co_4(\mu_4\text{-}O)(Me_2pzCO_2)_3$] ·~3 DMSO}$_n$ (1)

In a screw-capped Pyrex tube 20.6 mg ($7.0 \cdot 10^{-2}$ mmol) of $Co(NO_3)_2 \cdot 6\ H_2O$ and 10.0 mg ($7.0 \cdot 10^{-2}$ mmol) of HMe_2pzCO_2H were dissolved in 1.5 mL of a mixture of DMSO/DMF/MeOH (10:4:1). The solution was heated to 110 °C and then up to 120 °C within three days. The clear, deep-violet cubic crystals (Fig. S11) were filtered and washed three times with 10 mL of DMF. They were dried under a vacuum of 10^{-2} Torr and stored under inert atmosphere.

Yield: 40 mg (60 % based on ligand)

FTIR (ATR): 3216, 3010, 2920, 2340, 1706, 1543, 1507, 1477, 1421, 1393, 1369, 1289, 1172, 1107, 1069, 997, 950, 815, 803, 745, 712, 670, 617 cm^{-1} (see Fig. S12).

We note that meaningful elemental analyses of MOFs are difficult to obtain due to solvent loss and different sample states (different states of dryness vs. not dried).

A total of 860 electrons per 3100 $Å^3$ (compare with total potential solvent area volume of 3182 $Å^3$ calcd. by PLATON VOID) was squeezed by PLATON in the structure refinement of **1** which corresponds to ~107 electrons per $C_{18}H_{18}Co_4N_6O_7$ formula unit (Z = 8). One DMSO molecule provides 42 electrons.

In TG/DTA (see Fig. S13) the dried compound shows a first weight loss of 27.7% in a temperature range from 200 °C to 300 °C. This weight loss can be assiged to the loss of about 3 DMSO solvent molecules (theor. 26%). In the range from ~450 °C to 500 °C a second weight loss of ~39% takes place which is due to decomposition of the ligand.

For the cobalt complex a removal of solvent is easier than for the zinc complex with the same ligand because of the smaller DMSO molecule in {[$Co_4(\mu_4\text{-}O)(Me_2pzCO_2)_3$] ·~3 DMSO}$_n$ compared with the diethylformamide, DEF molecule in {[$Zn_4(\mu_4\text{-}O)(Me_2pzCO_2)_3$] ·~2 DEF}$_n$ (see. Fig. S16).

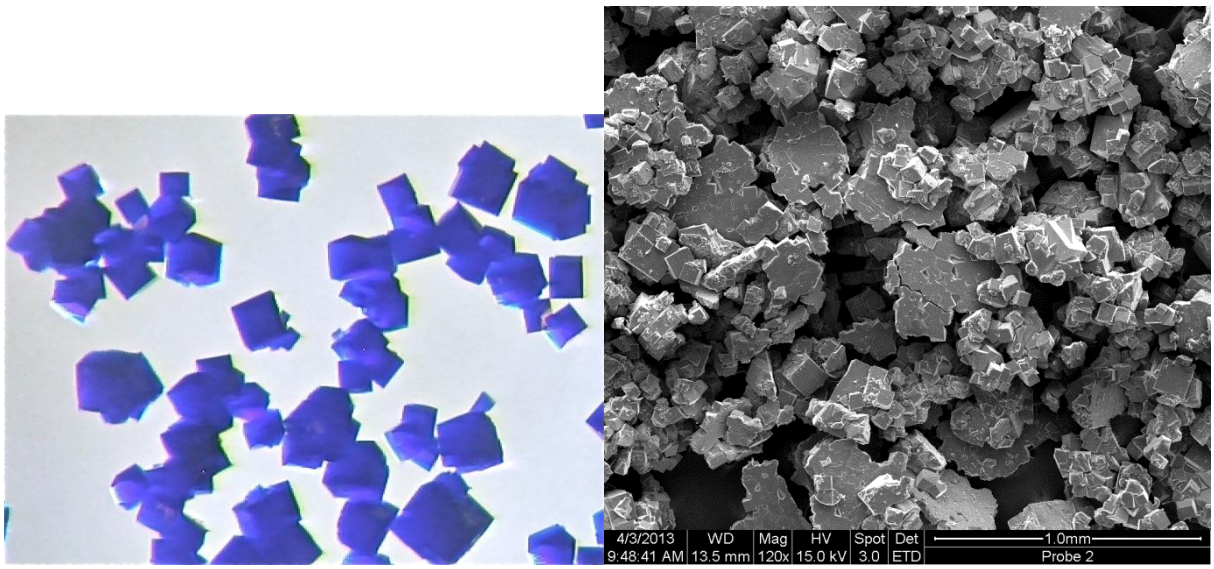

Fig. S11. Crystals of $\{[Co_4(\mu_4\text{-}O)(Me_2pzCO_2)_3] \cdot 3\ DMSO\}_n$ (**1**) by optical photography and scanning electron microscopy. The cubic shape of the crystals already hints at the cubic crystal system with space group F-43m.

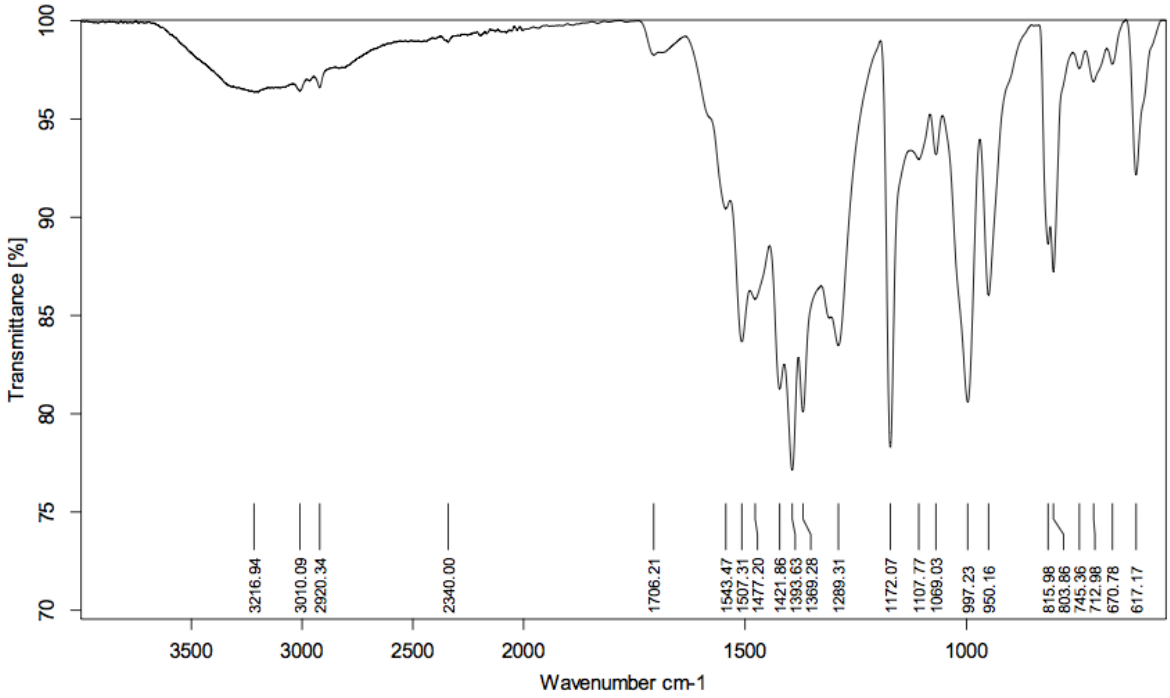

Fig. S12. FTIR (ATR) of compound $\{[Co_4(\mu_4\text{-}O)(Me_2pzCO_2)_3] \cdot \sim 3\ DMSO\}_n$ **1**.

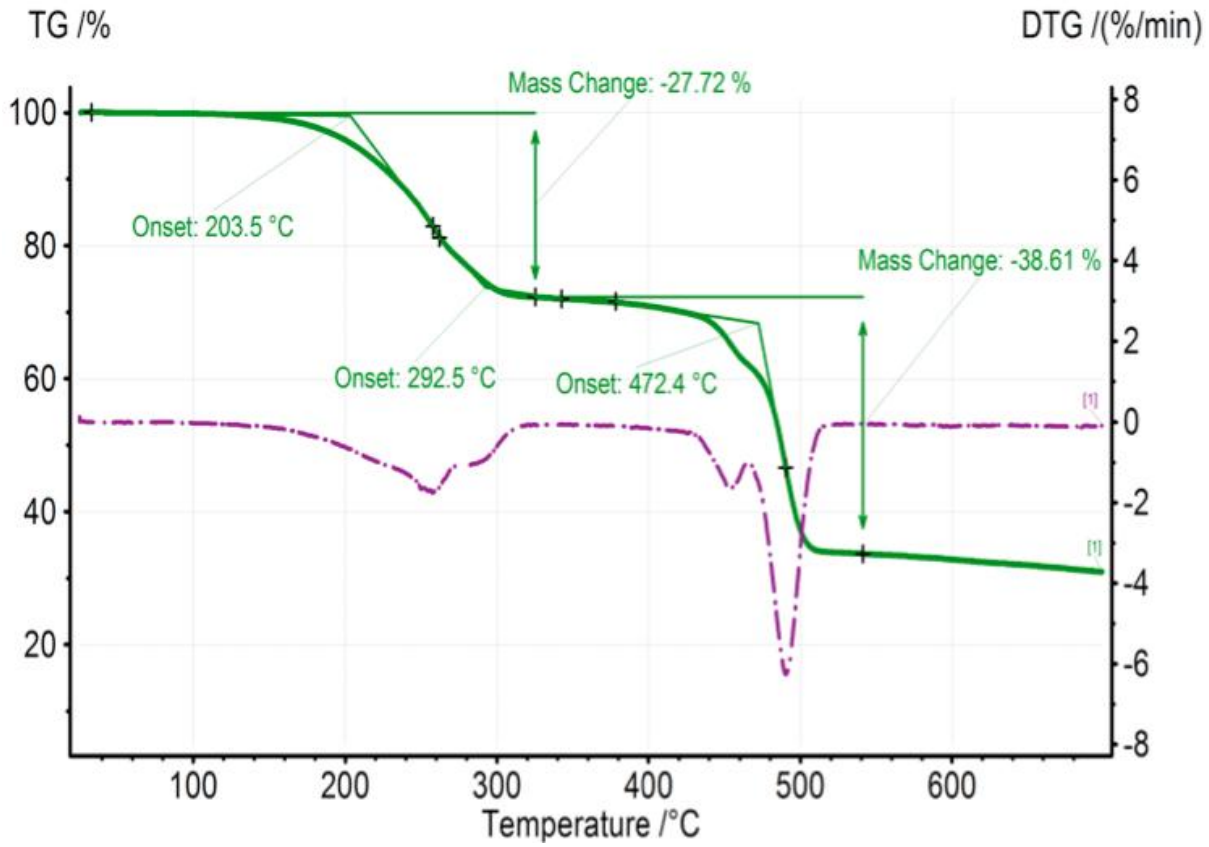

Fig. S13. TG/DTG of $\{[Co_4(\mu_4\text{-}O)(Me_2pzCO_2)_3]\cdot\sim 3\ DMSO\}_n$ (**1**)

$\{[Zn_4(\mu_4\text{-}O)(Me_2pzCO_2)_3]\cdot\sim 2\ DEF\}_n$ (2)

In a screw-capped Pyrex tube 1.13 g (0.28 mmol) of $Zn(NO_3)_2 \cdot 4\ H_2O$ and 0.3 g (0.14 mmol) of HMe_2pzCO_2H were dissolved in 30 mL of DEF. The clear solution was heated to 140 °C within two days and kept for another two days at this temperature. The clear yellowish cubic crystals (Fig. S14) were decanted and seperated from impurities by density difference using a mixture of bromoforme and methanol. After centrifugation the product was washed three times with 10 mL of DEF, dried under a vacuum of 10^{-2} Torr and stored under inert atmosphere.

Yield: 310 mg (22 % based on ligand)

FTIR (ATR): 2971, 2927, 1675, 1567, 1516, 1490, 1428, 1405, 1377, 1307, 1259, 1216, 1182, 1106, 1071, 1041, 994, 941, 820, 803, 667, 642, 620 cm^{-1} cm^{-1} (see Fig. S15).

We note that meaningful elemental analyses of MOFs are difficult to obtain due to solvent loss and different sample states (different states of dryness vs. not dried).

A total of 812 electrons per 3688 $Å^3$ (compare to total potential solvent area volume of 3737 $Å^3$ calcd. by PLATON VOID) was squeezed by PLATON in the structure refinement of **2** which corresponds to ~101 electrons per $C_{18}H_{18}N_6O_7Zn_4$ formula unit (Z = 8). One DEF molecule

provides 56 electrons.

In TG/DTA (see Fig. S16) the dried compound shows a small and continuous weight loss starting at 200 °C and which becomes more visible at 300 °C. This weight loss is assigned to high-boiling/low-volatile DEF crystal solvent molecules which have to escape through the narrow pores. The solvent weight loss continues into the ligand decomposition between 400 and 500 °C (cf. Fig. S13 for the ligand decomposition at the Co compound **1**).

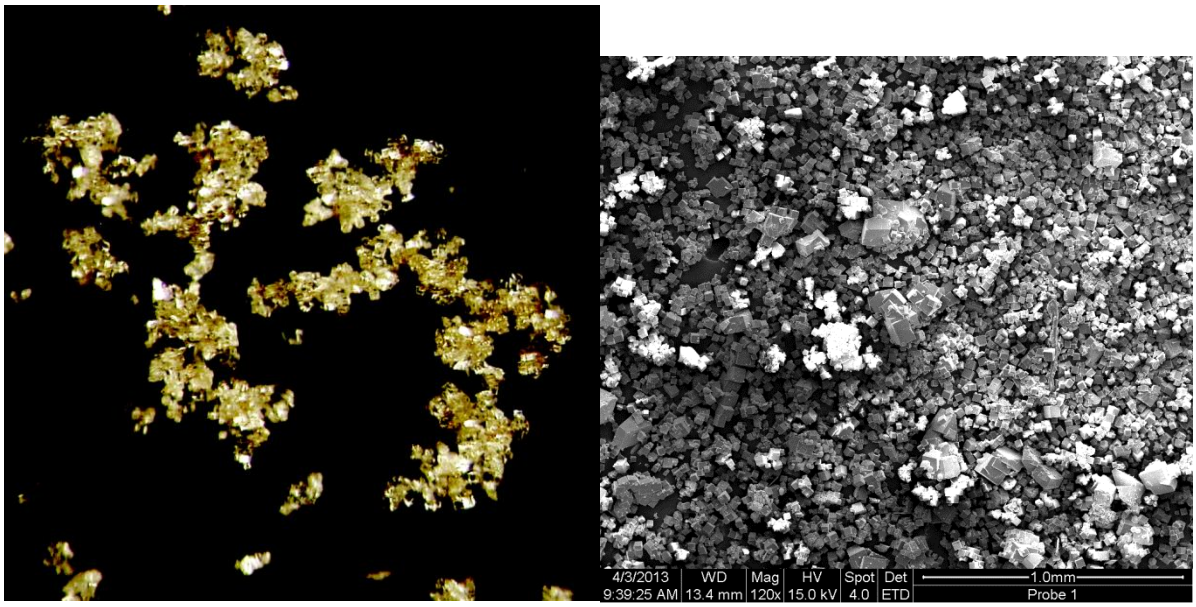

Fig. S14. Crystals of $\{[Zn_4(\mu_4\text{-}O)(Me_2pzCO_2)_3]\cdot\sim 2\ DEF\}_n$ (**2**) by optical photography and scanning electron microscopy. The cubic shape of the crystals already hints at the cubic crystal system with space group F-43m.

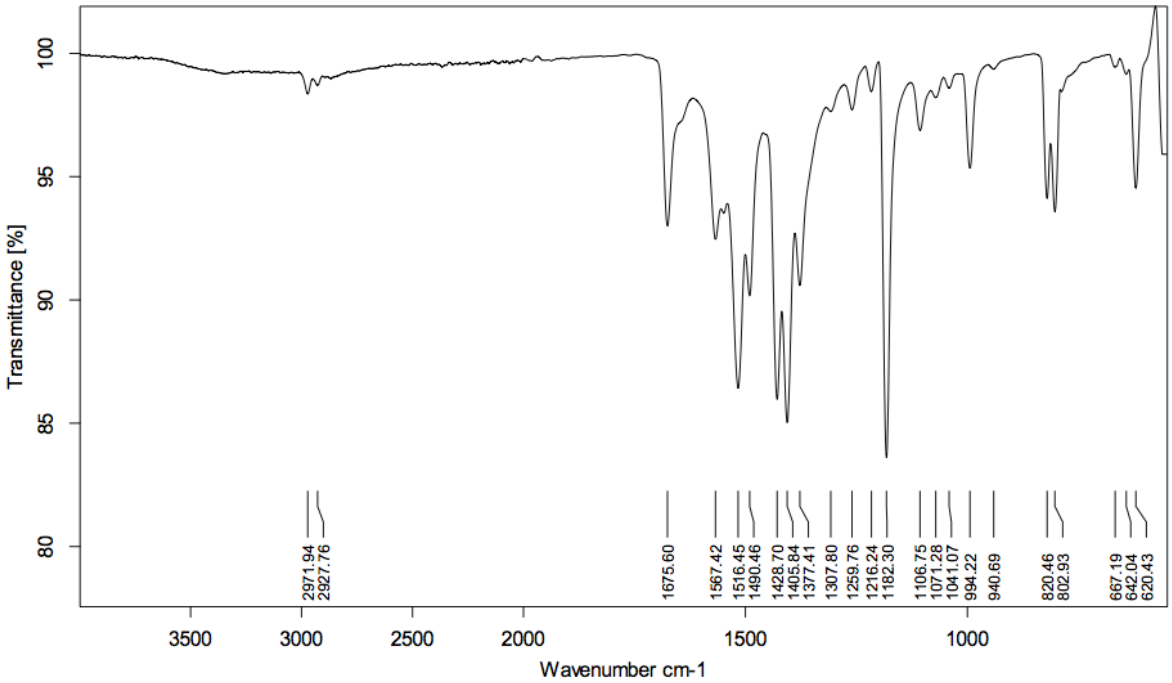

Fig. S15. FTIR (ATR) of compound $\{[Zn_4(\mu_4\text{-}O)(Me_2pzCO_2)_3]\cdot\sim 2\ DEF\}_n$ (**2**).

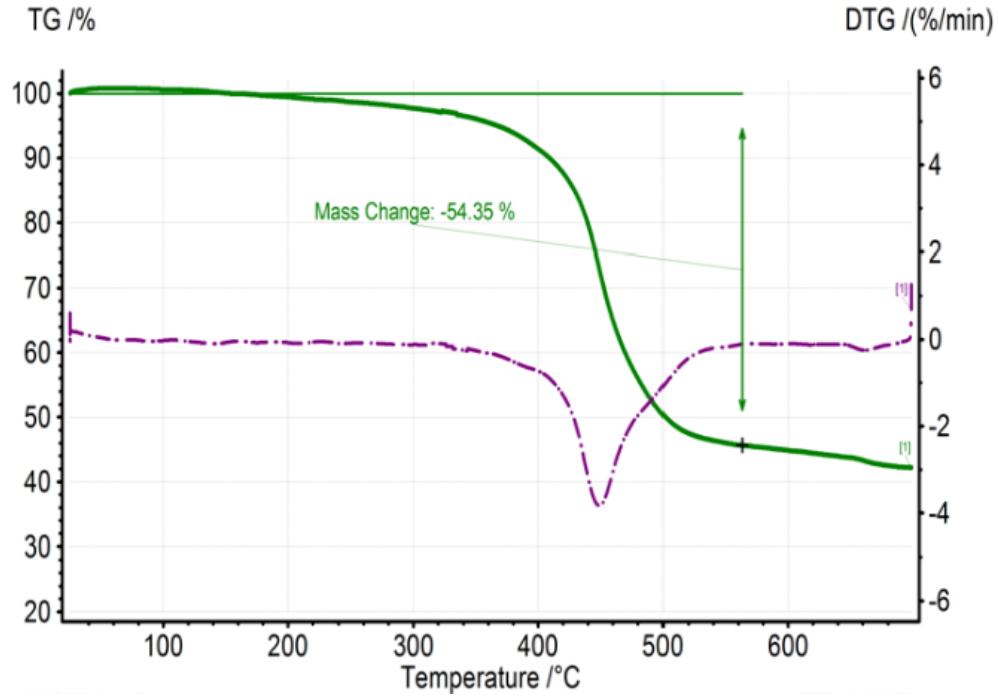

Fig. S16. TG/DTG of $\{[Zn_4(\mu_4\text{-}O)(Me_2pzCO_2)_3]\cdot\sim 2\ DEF\}_n$ (**2**).

{[$Co_4(\mu_4\text{-}O)(Me_2pzC_6H_4CO_2)_3$] ·~6 DMSO ·~6 H_2O ·~2 DMF}$_n$ (3)

In a screw-capped Pyrex tube 20.2 mg (0.07 mmol) of $Co(NO_3)_2 \cdot 6\ H_2O$ and 10.0 mg (0.046 mmol) of 3,5-dimethyl-4-(4-carboxyphenyl)-1*H*-pyrazole ($HMe_2pzC_6H_4CO_2H$) were dissolved in 1.5 mL of a mixture of DMSO/DMF/MeOH (10:4:1). The solution was then heated from 115 °C to 130 within three days and kept for another two day at this temperature. Deep-violet cubic crystals (Fig. S17) were formed which were filtered and washed three times with 5 mL portions of DMF. They were dried under a vacuum of 10^{-2} Torr and stored under inert atmosphere.

Yield: 50 mg (70 % based on ligand).

FTIR (ATR): 3326, 2933, 2829, 1586, 1545, 1400, 1303, 1178, 1103, 1030, 1015, 867, 789, 716, 665, 634, 607 cm^{-1} (see Fig. S18).

We note that meaningful elemental analyses of MOFs are difficult to obtain due to solvent loss and different sample states (different states of dryness vs. not dried).

A total of 749 electrons per 2107 $Å^3$ was squeezed by PLATON in the structure refinement of **3** which corresponds to an appropriate number of solvent molecules per unit cell (Z = 1). There is one formula unit [$Co_4(\mu_4\text{-}O)(Me_2pzC_6H_4CO_2)_3$], $C_{36}H_{30}Co_4N_6O_7$ per unit cell (Z = 1). The possible solvent molecules provide the following number of electrons:

molecule	number of electrons
DMSO, $(CH_3)_2SO$	42
H_2O	10
DMF, $(CH_3)_2NCHO$	40
MeOH, CH_3OH	18

TG/DTA (see Fig. S19) shows two weight losses of 9.32 and 12.0 wt% up to 300 °C.

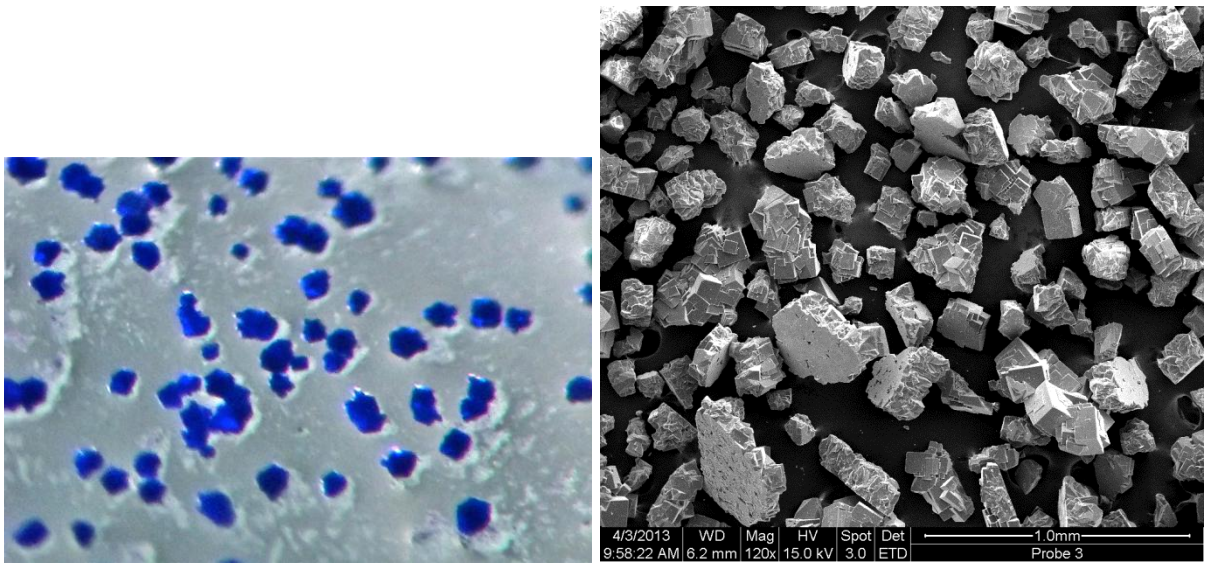

Fig. S17. Crystals of {[$Co_4(\mu_4\text{-}O)(Me_2pzC_6H_4CO_2)_3$] ·solvent}$_n$ (**3**) by optical photography and scanning electron microscopy. The cubic shape of the crystals already hints at a near cubic crystal system with the orthorhombic space group P222 and nearly identical cell constants *a* = 14.242(3), *b* = 14.278(3), *c* = 14.332(4) Å (see Table 2).

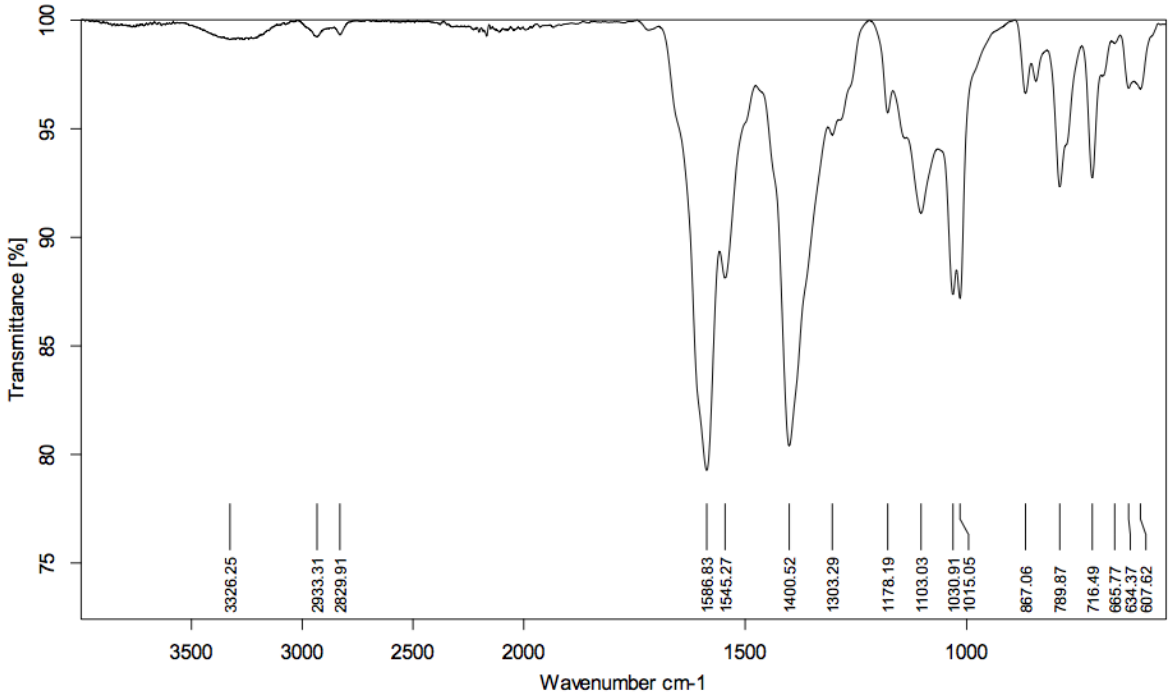

Fig. S18. FTIR (ATR) of compound {[$Co_4(\mu_4\text{-}O)(Me_2pzC_6H_4CO_2)_3$] ·solvent}$_n$ (**3**).

A TGA of the dried compound shows a series of steady weight losses from the very beginning and up to over 500 °C with only narrow plateaus in between (Fig. S19). The first immediate mass loss of ~9% ends at ~100 °C where the second mass loss of ~12% starts which continous to about 300 °C or perhaps even 400 °C. These two differentiated weight loss ranges can be assigned to at least two different types of crystal solvent because of the three (four) different

solvents DMSO, DMF, MeOH (and water) present in the crystallization process. Up to 100 °C methanol and water molecules may leave the compound. The weight loss from over 100 °C to ~400 °C indicates the removal of higher boiling/less volatile DMSO and DMF molecules. Around 400 °C a steeper mass loss of ~14% starts, immediately followed by another steep mass loss of ~19.5%. These two mass losses are attributed to ligand decomposition (Fig. S19).

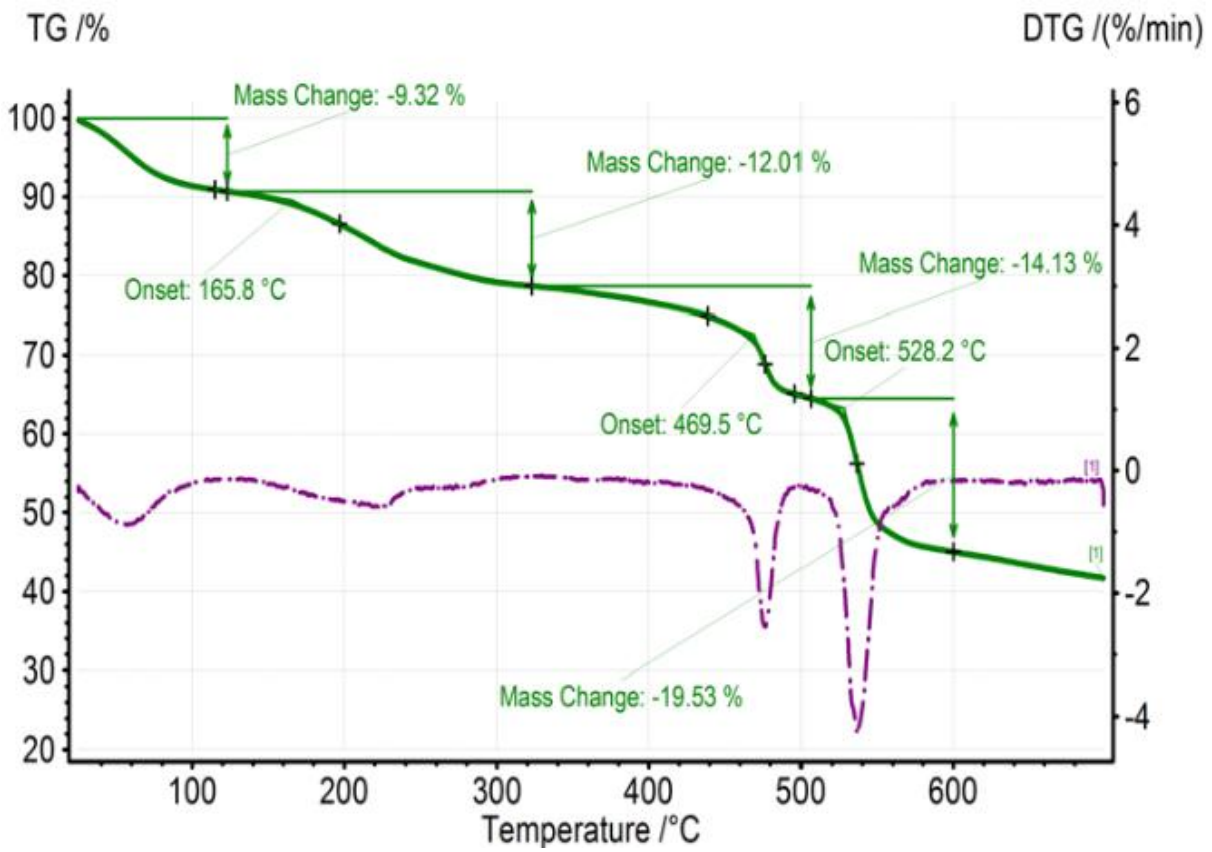

Fig. S19. TG/DTG of $\{[Co_4(\mu_4\text{-}O)(Me_2pzC_6H_4CO_2)_3]\cdot solvent\}_n$ (**3**)

{[$Zn_4(\mu_4\text{-}O)(Me_2pzC_6H_4CO_2)_3$] ·~3 DEF}$_n$ (4)

In a screw-capped Pyrex tube 18.0 mg (0.07 mmol) $Zn(NO_3)_2 \cdot 4\ H_2O$ and 10.0 mg (0.046 mmol) 3,5-dimethyl-4-(4-carboxyphenyl)-1*H*-pyrazole ($HMe_2pzC_6H_4CO_2H$) were dissolved in 1.5 mL DEF. The solution was then heated to 140 °C within three days and kept for another two day at this temperature. Clear cubic crystals (Fig. S20) were formed which were filtered and washed three times with 5 mL portions of DEF. They were dried under a vacuum of 10^{-2} Torr and stored under inert atmosphere.Yield: 11.7 mg (60 % based on ligand).

FTIR (ATR): 2972, 2931, 2869, 1671, 1608, 1583, 1534, 1491, 1410, 1335, 1307, 1286, 1261, 1216, 1183, 1107, 1030, 1013, 941, 870, 850, 806, 784, 717, 699, 664, 637, 606, 588, 560 cm^{-1} (see Fig. S21).

We note that meaningful elemental analyses of MOFs are difficult to obtain due to solvent loss and different sample states (different states of dryness vs. not dried).

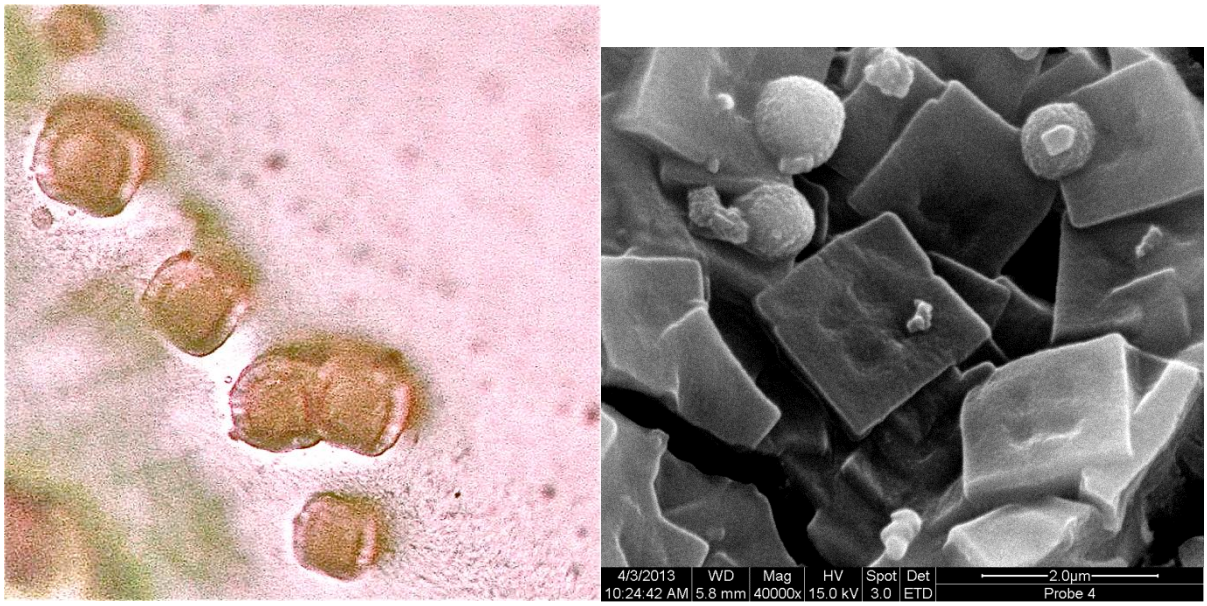

Fig. S20. Crystals of {[$Zn_4(\mu_4\text{-}O)(Me_2pzC_6H_4CO_2)_3$] ·~3 DEF}$_n$ (**4**) by optical photography and scanning electron microscopy. The cubic shape of the crystals already hints at a near cubic crystal system most likely with the same orthorhombic space group P222 and nearly identical cell constants as for **3**.

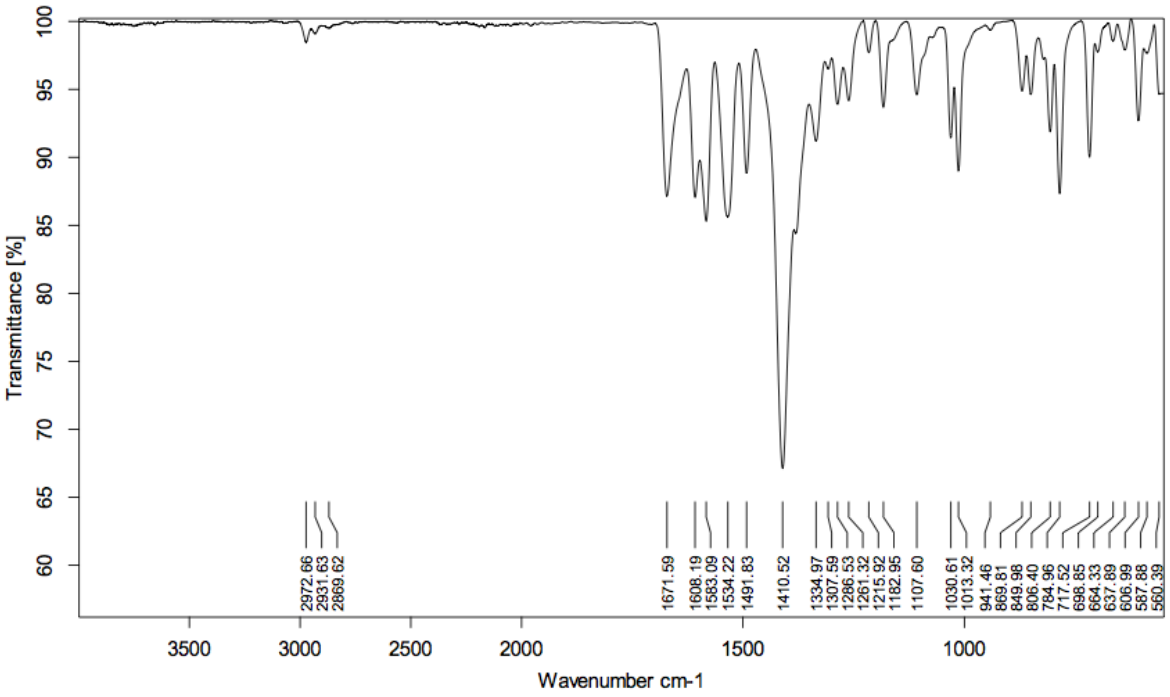

Fig. S21. FTIR (ATR) of compound $\{[Zn_4(\mu_4\text{-}O)(Me_2pzC_6H_4CO_2)_3]\cdot\sim 3\ DEF\}_n$ (**4**).

A TGA of the complex shows a weight loss of ~28% from the very beginning up to 200 °C (Fig. S22). This immediate weight loss can be correlated to about three DEF molecules (theor. 25%). From 200 °C to ~450 °C the framework appears thermally stable. Over 450 °C the ligand decomposes with a weight loss of ~40%.

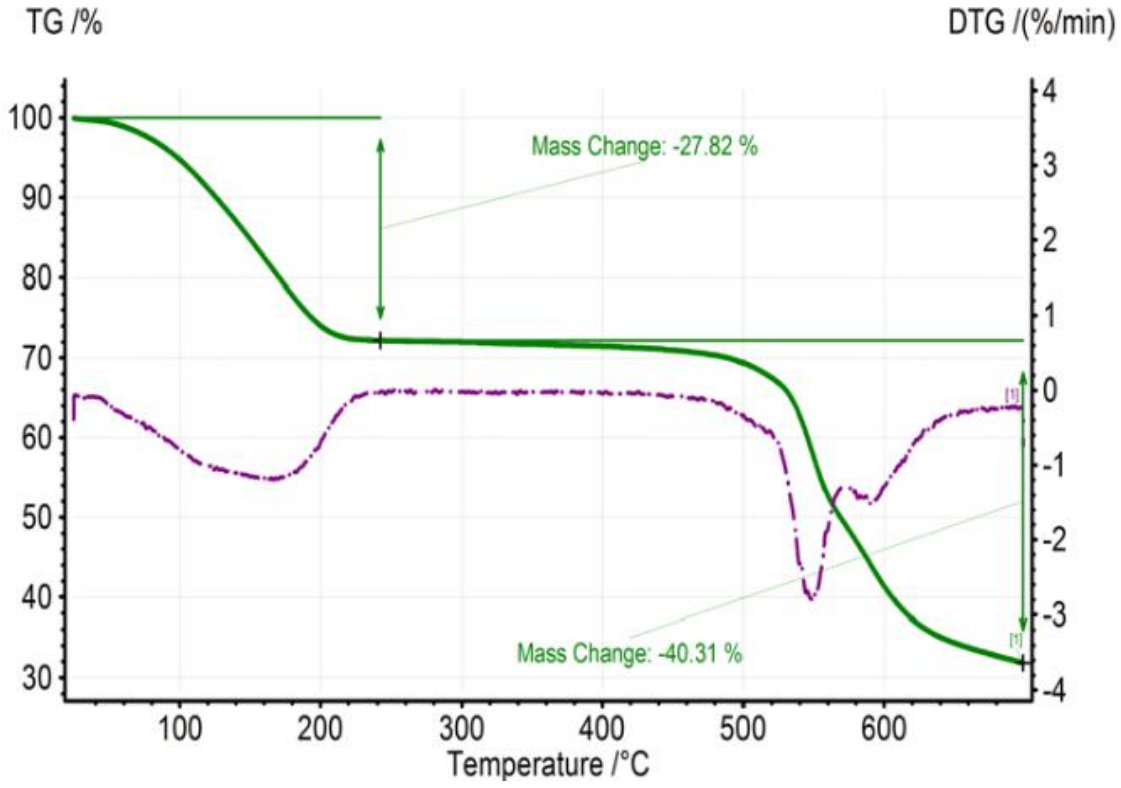

Fig. S22. TG/DTG of $\{[Zn_4(\mu_4\text{-}O)(Me_2pzC_6H_4CO_2)_3]\cdot\sim 3\ DEF\}_n$ (**4**).

Additional figures of building blocks and packing diagrams

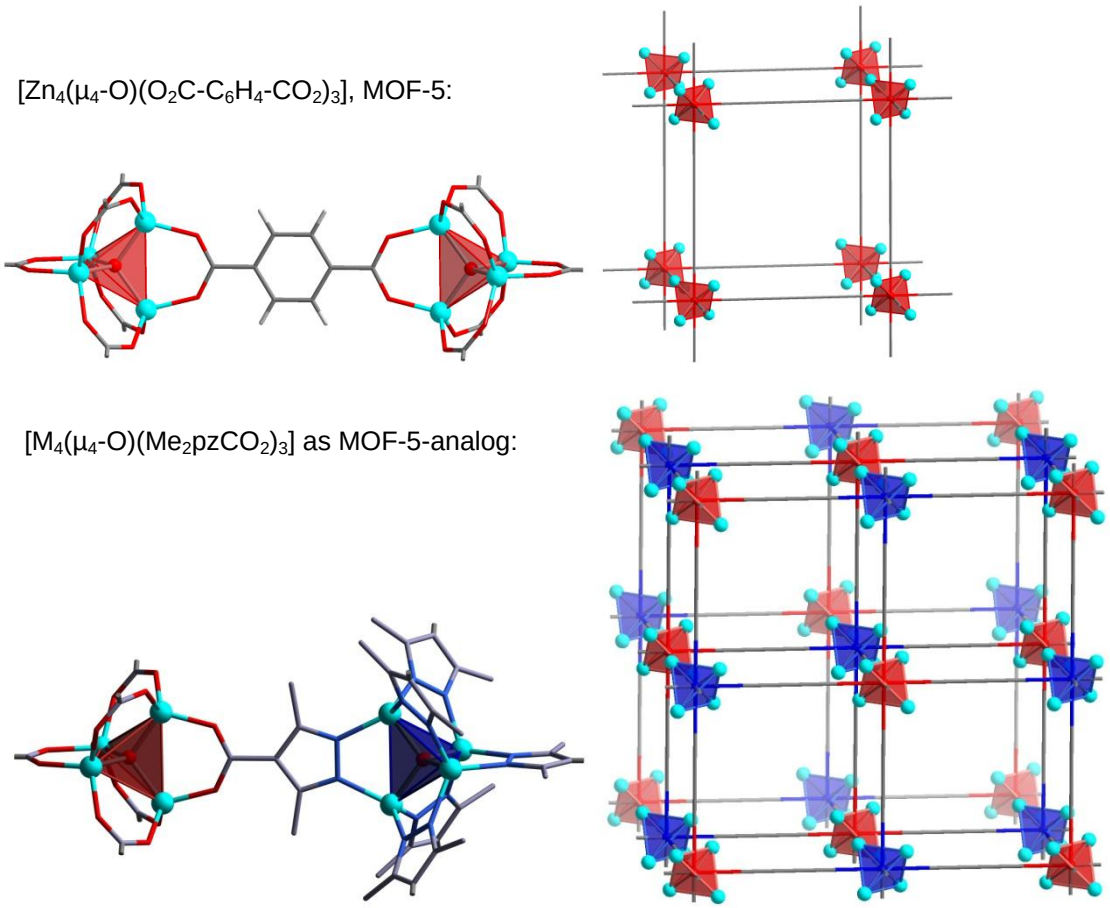

Fig. S23. Building blocks and cubic *pcu-a* frameworks in MOF-5 and **1** (M = Co) or **2** (M = Zn) to illustrate the analogy. Colors: oxygen atoms red, nitrogen atoms blue, metal atoms cyan, carbon atoms grey, hydrogen atoms (in MOF-5) light grey.

The fixed alternating canting of the dimethylpyrazolate ring plane (cf. Fig. S24a) leads to alternating small (van der Waals diameter, Ø ~6 Å) and large pores (Ø ~11 Å) connected by small channels or pore apertures (Ø ~2.8 Å) (Fig. 24b). Failure of N_2 adsorption in **1** and **2** is presumably due to activated diffusion effects associated with the low thermal energy of N_2 relative to the high barrier for diffusion through the small 2.8-diameter pore apertures (cf. Fig. S24b). In other words, at slow thermal motion at 77 K the N_2 molecule will statistically only seldom approach the small pore aperture with the correct orientation for penetration, that is, at right angle with its molecule axis.

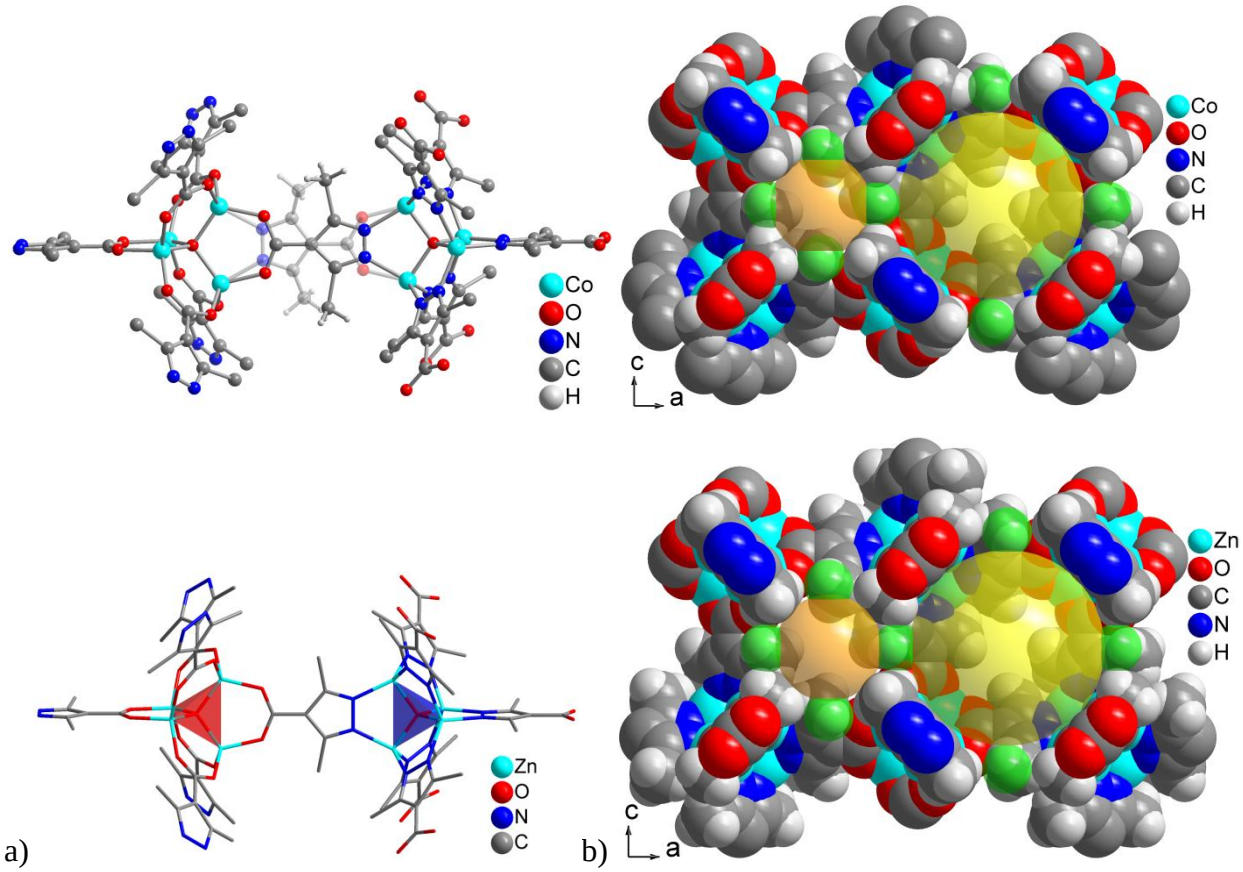

Fig. S24. Building units (a) in $[M_4(\mu_4\text{-}O)(Me_2pzCO_2)_3]$ (M = Co, **1**; Zn, **2**). Space-filling plots for M = Co and Zn in (b) show the alternating small (transparent orange sphere, diameter, Ø = 6 Å) and large (yellow sphere, Ø = 11 Å) cavities due to the alternating pyrazolate plane orientation with pore apertures (green spheres, Ø = 2.8 Å) in between.

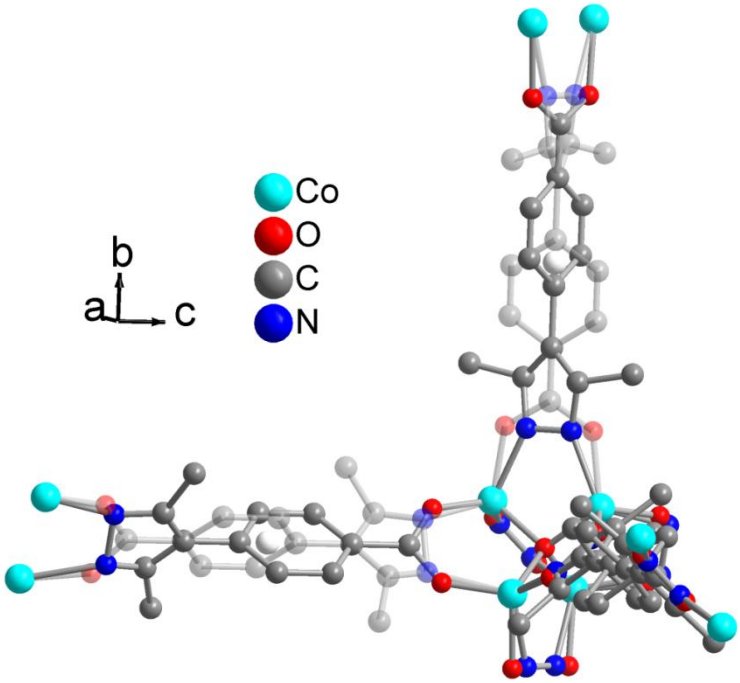

Fig. S25. Schematic presentation of the idealized crystallographically induced ligand disorder in **3** by showing two of the three symmetry-independent pyrazolate-benzoate ligands. As a visual aid one of the symmetry-related disordered orientations is shown transparent. The crystallographically-induced disorder is due to C2-axes passing through the white atom at the ligand center and running parallel to the unit-cell axes. Hydrogen atoms are not shown.

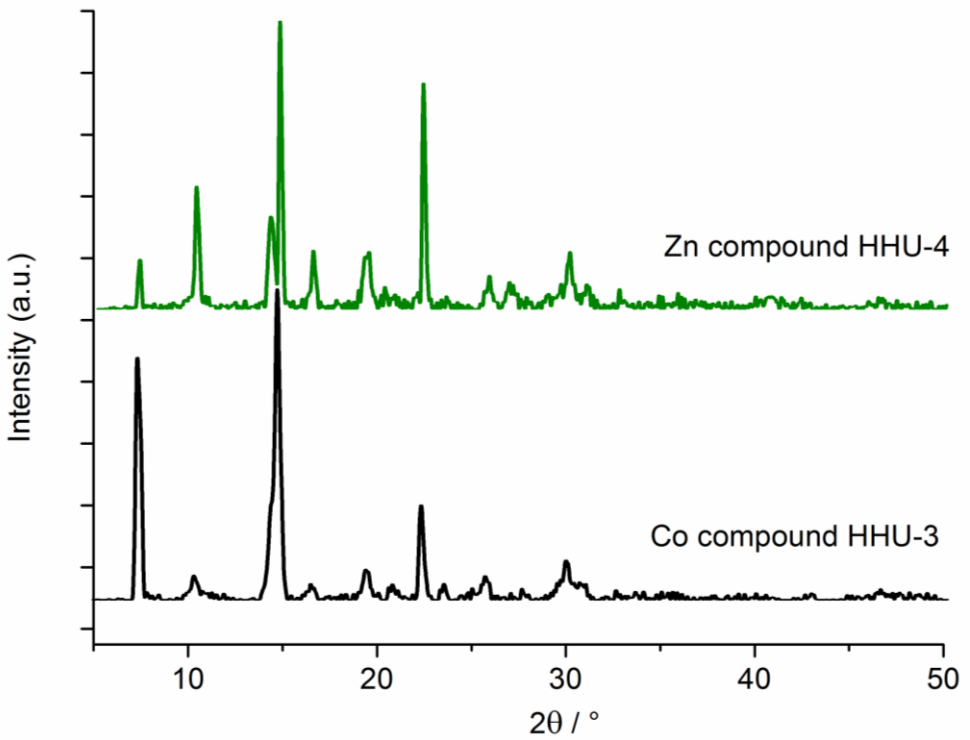

Fig. S26. Powder X-ray diffractograms of $[M_4(\mu_4\text{-}O)(Me_2pzC_6H_4CO_2)_3]$ (M = Co, **3**; Zn, **4**). Diffractograms were obtained on flat layer sample holders where at low angle the beam spot is strongly broadened so that only a fraction of the reflected radiation reaches the detector which leads to the low relative intensities measured at $2\theta < 10°$.

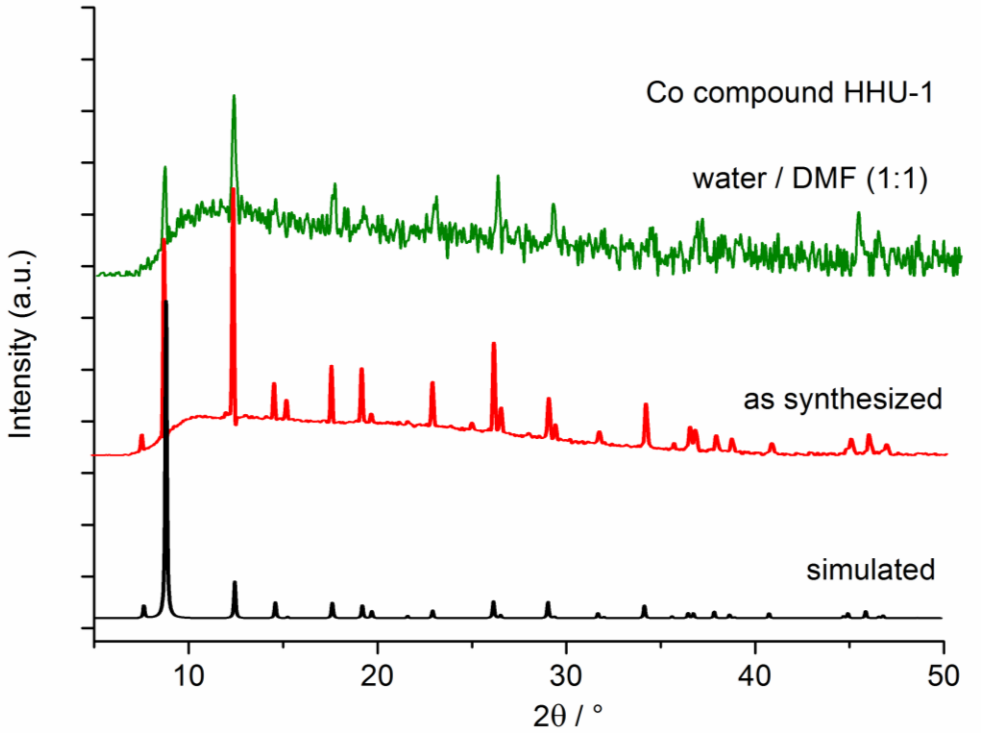

Fig. S27. Powder X-ray diffractograms of $[Co_4(\mu_4\text{-}O)(Me_2pzCO_2)_3]$ (**1**) before (as synthesized) and after the water stability test in water/DMF (1:1 volumetric mixture). The simulated diffractogram is based on the X-ray data refinement.
Diffractograms were obtained on flat layer sample holders where at low angle the beam spot is strongly broadened so that only a fraction of the reflected radiation reaches the detector which leads to the low relative intensities measured at $2\theta < 10°$. Diffractograms for Co compounds often have a high background because of Co-based X-ray fluorescence (see Daugherty, K. E.; Robinson, R. J.; Mueller, J. I. *Analytical Chemistry* **1964**, 36, 1869–1870.)

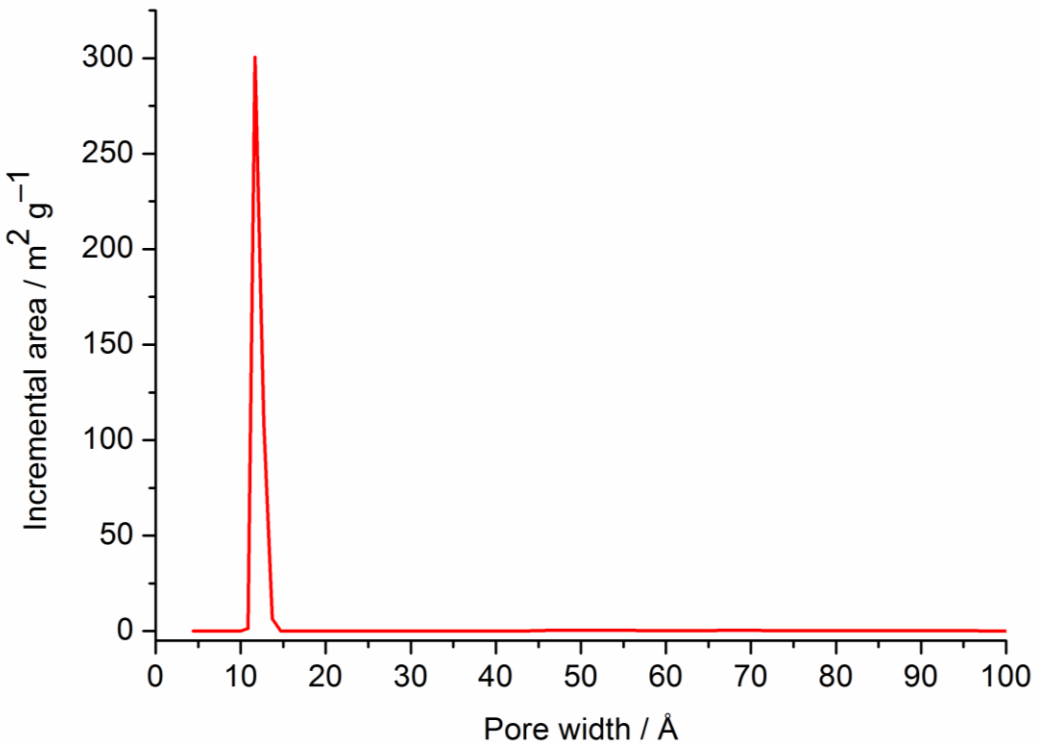

Fig. S28a. Pore size distribution curve of $\{[Co_4(\mu_4\text{-}O)(Me_2pzCO_2)_3]\}_n$ (activated **1**) from DFT calculation (Ar on carbon, slit based model) based on argon adorption isotherm (cf. Fig. 4).

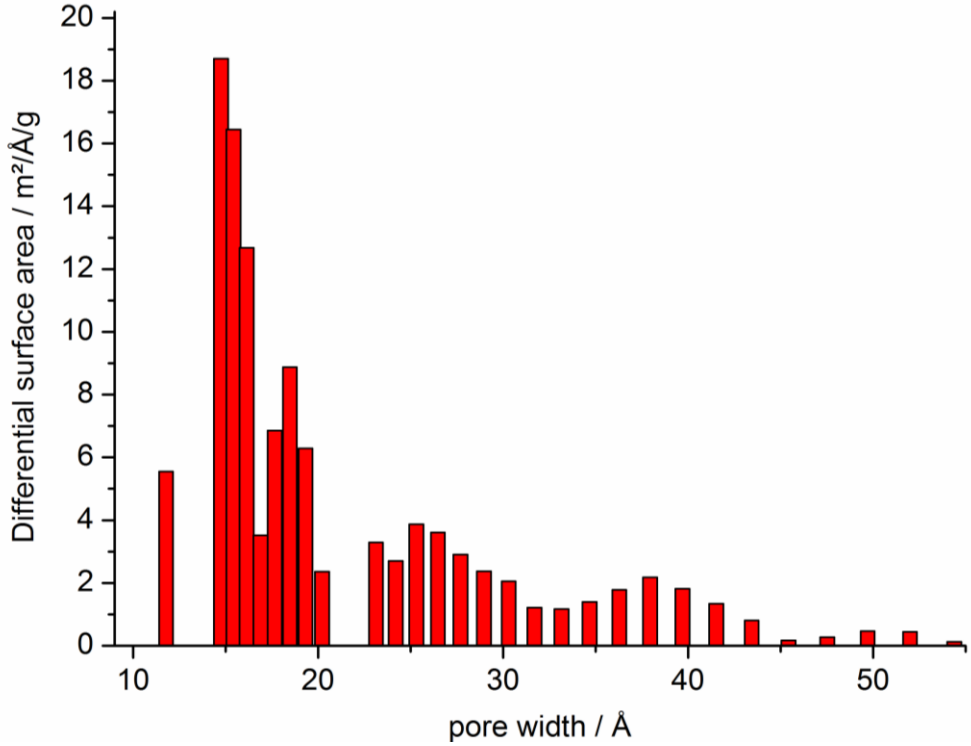

Fig. S28b. Differential surface area curve of $\{[Co_4(\mu_4\text{-}O)(Me_2pzC_6H_4CO_2)_3]\}_n$ (activated **3**) from DFT calculation (N_2 at 77 K on carbon, slit pore, NLDFT equilibrium model) based on N_2 adorption isotherm (cf. Fig. 6).

Hydrogen, carbon dioxide and methane gas sorption studies

From two adsorption isotherms acquired at different temperatures T_1 and T_2 (Fig. 5b), the differential heat of adsorption $\Delta H_{ads,diff}$ can be calculated for any amount of adsorbed substance after determining the required relative pressures p_1 and p_2. A modified form of the Clausius-Clapeyron equation is used (eq (1)).[4] $\Delta H_{ads,diff}$ was calculated over the whole adsorption range from the 77 K and 87 K isotherms for H_2 in **1** (Fig. 5b).

$$\Delta H_{ads,diff} = -Rln\left(\frac{p_2}{p_1}\right)\frac{T_1T_2}{T_2-T_1} \qquad (1)$$

The heat of adsorption for H_2 in **1** is determined to 5-6 kJ/mol. The increase with coverage is explained by the sequential filling of the large cavities, small cavities and eventually the channel volume with increasing adsorbate–surface interactions.

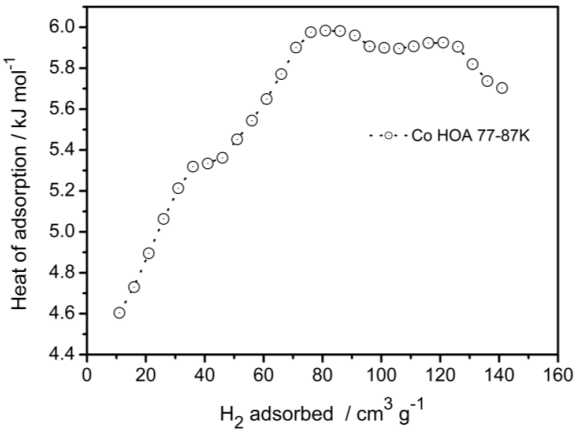

Fig. S29. Heat of adsorption for H_2 in **1** at 77-87 K.

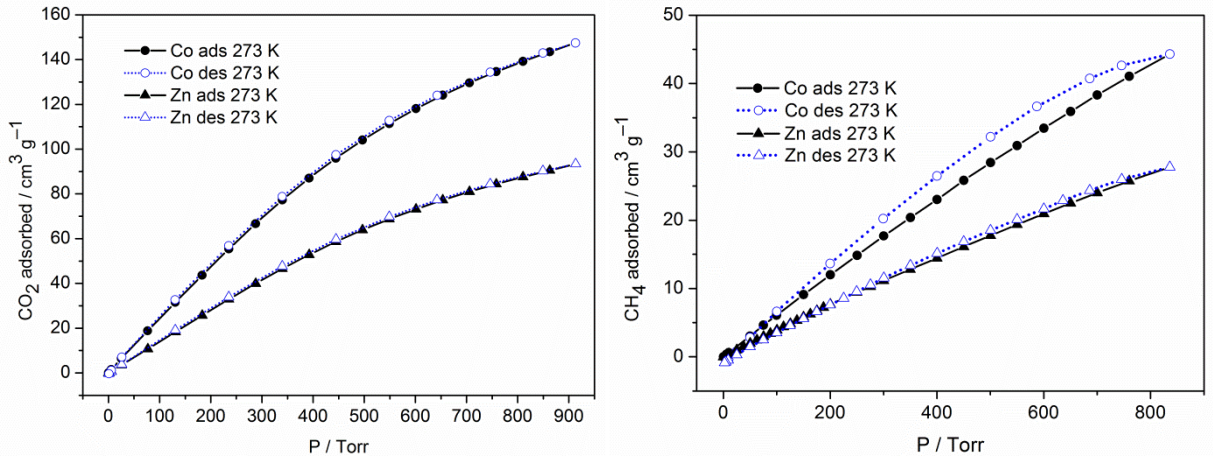

(a) (b)

Fig. S30. (a) CO_2 and (b) CH_4 sorption isotherms for **1** (Co) and **2** (Zn).

4 F. Rouquerol, J. Rouquerol and K. Sing, *Adsorption by powders and porous solids*, (F. Rouquerol, J. Rouquerol, K. Sing, Eds.), Academic Press, San Diego, 1999, vol. 11.

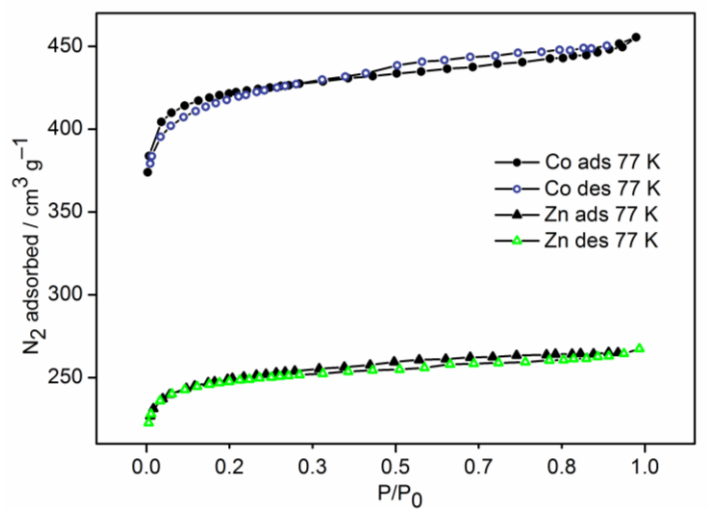

Fig. S31. N_2 sorption isotherms for **3** (Co) and **4** (Zn).

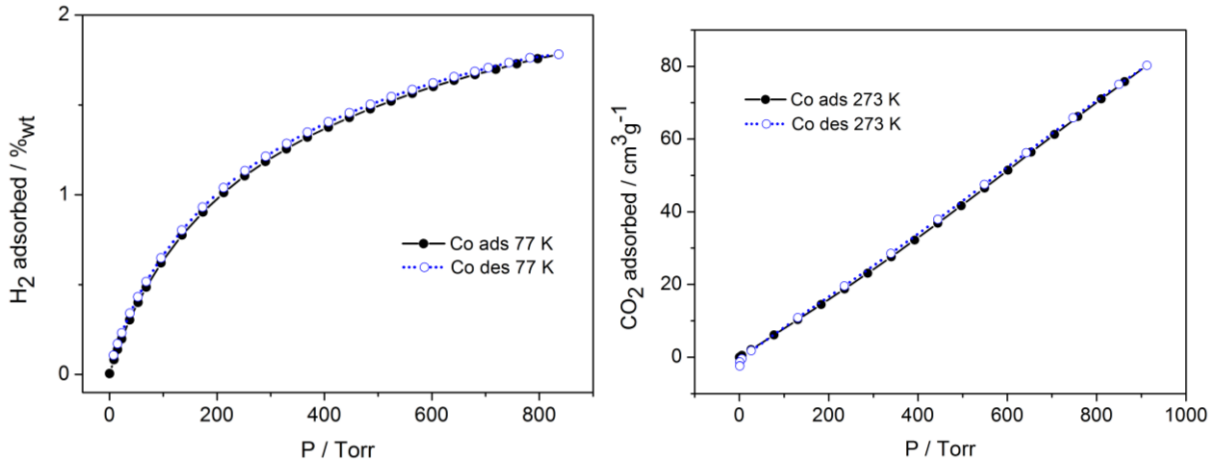

(a) (b)

Fig. S32. (a) H_2 and (b) CO_2 sorption isotherms for **3** (Co).

Table S1 Porosity data for **3** and **4** from N_2 isotherms at 77 K.

Compd	S_{BET} [a] (m^2/g)	S_{Lang} (m^2/g)	V_{tot} [b] (cm^3/g)
3	1072	1195	0.44
4	980	1063	0.41

[a] Calculated BET surface area over the pressure range 0.01-0.05 P/P_0; [b] total pore volume at P/P_0 = 0.95.

Gas selectivity

The ratio of the initial slopes in the Henry region of the adsorption isotherms (Fig. S33, Fig. S34)[5,6] determines the selectivities exhibited by **1** and **2** for adsorption of CO_2 over CH_4. **1** shows a selectivity ratio for CO_2:CH_4 of 4:1 at 273 K. The selectivity does not only depend on the size of the gas components (kinetic diameter: CO_2 3.3 Å, CH_4 3.8) but also on the polarizability of the surface and of the gas components.

Selectivities were estimated from the ratio of the initial slopes in the Henry region of the adsorption isotherms (Table S2).

Table S2 Initial slopes of adsorption isotherms and selectivities for CO_2:N_2 and CO_2:CH_4 at 273.

	initial slopes for gas adsorption isotherms	
Compounds	CO_2	CH_4
1 (Co)	0.2465	0.06146
2 (Zn)	0.1398	0.03913
	gas selectivities	
	CO_2:CH_4 selectivity at 273 K	
1 (Co)	~4:1	
2 (Zn)	~3.5:1	

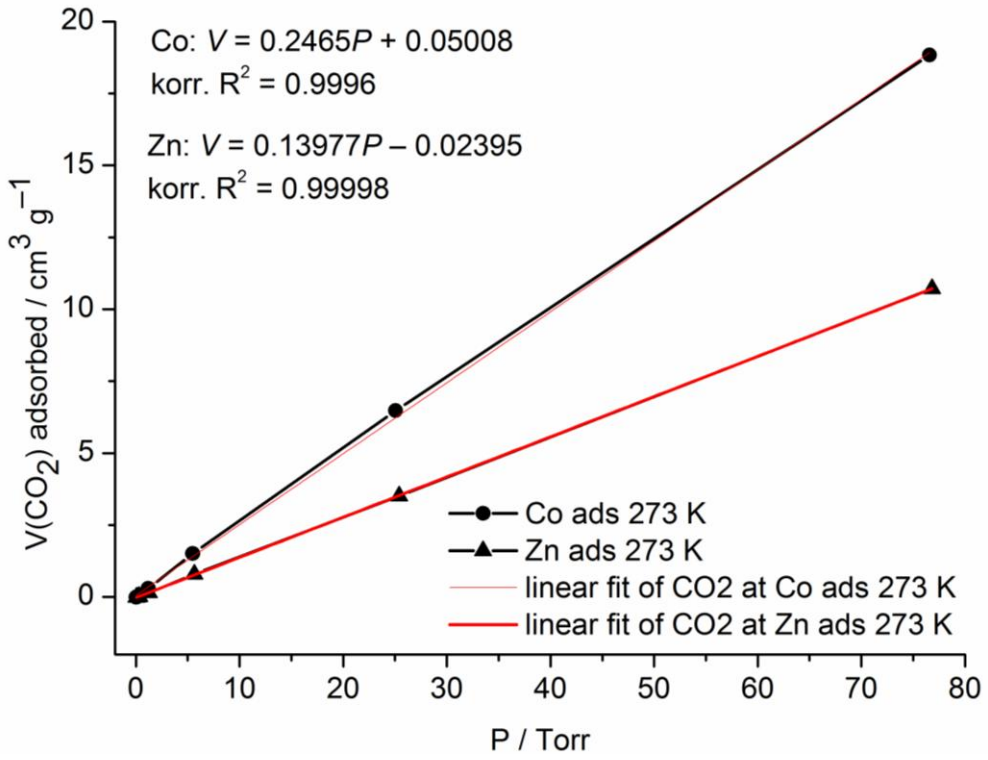

Fig. S33. The initial slope in the Henry region of the adsorption isotherms of CO_2 of **1** and **2** at 273 K.

5 V. Abetz, T. Brinkmann, M. Dijkstra, K. Ebert, D. Fritsch, K. Ohlrogge, D. Paul, K. V. Peinemann, S. Pereira-Nunes, N. Scharnagl and M. Schossig, *AIChE J.*, **2006**, *8*, 328-358.

6 Y.-S. Bae, O. K. Farha, A. M. Spokoyny, C. A. Mirkin, J. T. Hupp and R. Q. Snurr, *Chem. Commun.*, **2008**, 4135-4137.

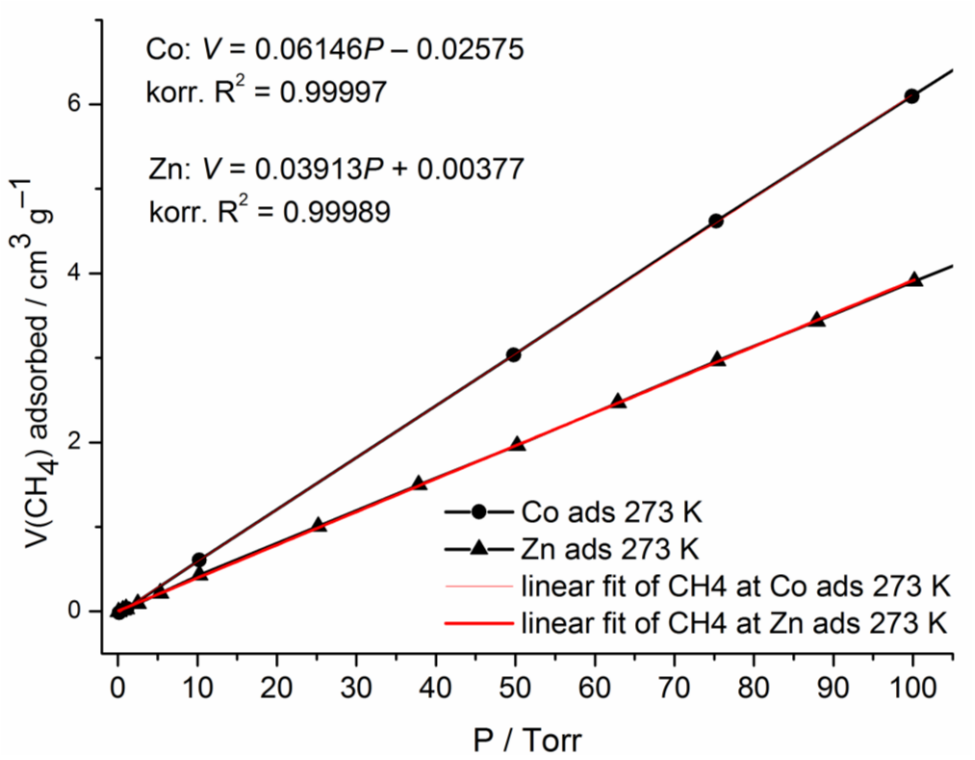

Fig. S34. The initial slope in the Henry region of the sorption isotherms of CH_4 of **1** and **2** at 273 K.